Computational Materials Science 200 (2021) 110831

Contents lists available at ScienceDirect

Computational Materials Science

journal homepage: www.elsevier.com/locate/commatsci

Yielding transition in stable glasses periodically deformed at finite temperature

Nikolai V. Priezjev *

Department of Mechanical and Materials Engineering, Wright State University, Dayton, OH 45435, United States of America
National Research University Higher School of Economics, Moscow 101000, Russia

ARTICLE INFO

Keywords:
Metallic glasses
Thermo-mechanical processing
Yielding transition
Oscillatory shear deformation
Molecular dynamics simulations

ABSTRACT

The effect of glass stability on the yielding transition and mechanical properties of periodically deformed binary glasses is investigated using molecular dynamics simulations. We consider a binary mixture first slowly cooled below the glass transition temperature and then mechanically annealed to deeper energy states via small-amplitude oscillatory shear deformation. We show that upon increasing glass stability, the shear modulus and the yielding peak during startup continuous deformation increase towards plateau levels. It is found that during the strain amplitude sweep, the yielding transition occurs at higher amplitudes and it becomes more abrupt in deeply annealed glasses. The processes of initiation and formation of a shear band are elucidated via the spatiotemporal analysis of nonaffine displacements of atoms. These results are important for thermo-mechanical processing of highly stable amorphous alloys.

1. Introduction

Understanding the relationship between the atomic structure and macroscopic properties of metallic glasses is important for a number of structural and biomedical applications [1–3]. It is well known that plastic deformation in disordered materials involves collective rearrangements of groups of atoms or shear transformations [4,5]. Often cases, an improvement in mechanical and physical properties of metallic glasses can be achieved via thermo-mechanical processing that relocates the disordered systems in a broad range of energy states [6]. Common examples include high-pressure torsion, cold rolling, wire drawing, irradiation, elastostatic loading, as well as surface treatments like shot peening [6]. Here, we highlight a recent discovery that thermal cycling between the room and cryogenic temperatures can lead to rejuvenation of metallic glasses due to heterogeneous thermal expansion [7–18]. Remarkably, it was also recently demonstrated experimentally and by means of atomistic simulations that cooling across the glass transition temperature under applied stress rejuvenates amorphous alloys and increases their ductility [19,20]. However, despite extensive efforts aimed at exploring the operational parameter space in order to extend the range of glassy state, the optimization of processing routes remains a difficult task.

During the last decade, the relaxation, rejuvenation and critical phenomena in disordered alloys subjected to time periodic deformation were extensively studied using atomistic and mesoscale simulations [21–51]. The modeling efforts can be broadly divided into two categories; namely, simulations either at zero temperature using oscillatory athermal quasistatic shear deformation protocol or at finite temperatures and non-zero strain rates. In the former case, it was found that, following a number of transient cycles, the trajectories of all atoms become exactly reversible after one or more cycles, provided that the strain amplitude is below a critical value [24,25]. Moreover, the number of cycles to reach a 'limit cycle' increases upon approaching the critical strain amplitude [23,24,52]. In the presence of thermal fluctuations, atoms do not follow exactly the same trajectories, and disordered solids might continue structural relaxation, or 'mechanical annealing', during thousands of subyield loading cycles [34,36,39]. Interestingly, it was recently shown that oscillatory shear deformation can lead to rejuvenation without formation of a shear band if the strain amplitude is only once in a while increased above a critical value [49]. On the other hand, the yielding transition is accompanied by strain localization, and the number of transient cycles depends on the initial glass state and strain amplitude [31,32,35,38,42,45], among other factors. Furthermore, it was found that highly stable glasses do not further relax during subyield loading, while they yield discontinuously at the critical strain amplitude, which in turn increases with the degree of annealing [44,48]. At finite temperatures, however, the precise determination of the critical strain amplitude and its dependence on the glass stability remains a challenging problem.

In this paper, the yielding transition in stable glasses under oscillatory shear deformation is studied by means of molecular dynamics

* Correspondence to: Department of Mechanical and Materials Engineering, Wright State University, Dayton, OH 45435, United States of America.
E-mail address: nikolai.priezjev@wright.edu.

https://doi.org/10.1016/j.commatsci.2021.110831
Received 22 May 2021; Received in revised form 1 August 2021; Accepted 23 August 2021

simulations. We consider a binary glass first mechanically annealed below the glass transition temperature and then cooled deep into the glass phase. We find that under startup continuous deformation, the shear modulus and the peak value of the stress overshoot increase towards plateau levels in more stable glasses. In the case of periodic loading, we introduce a shear deformation protocol with gradually varying strain amplitude in order to determine the critical strain amplitude at finite temperature. It will be shown that the yielding transition occurs at higher critical strain amplitudes and it becomes more abrupt in glasses annealed to deeper energy levels.

This paper is organized as follows. The details of atomistic simulations, mechanical annealing, and shear deformation protocol are described in the next section. The variation of the potential energy during mechanical annealing and yielding transition, as well as systems snapshots near the critical strain amplitude are presented in Section 3. The results are briefly summarized in the last section.

2. Molecular dynamics (MD) simulations

In the present study, the amorphous alloy was represented via the binary (80:20) Lennard-Jones (LJ) mixture model, which was first introduced by Kob and Andersen (KA) [53]. In this model, the unlike atoms have strongly non-additive interaction, which prevents crystallization upon cooling below the glass transition temperature [53]. The parametrization of the KA model is similar to the one used by Weber and Stillinger to study the amorphous metal–metalloid alloy $Ni_{80}P_{20}$ [54]. In the KA model, the interaction between atoms of types $\alpha, \beta = A, B$ is described by the LJ potential:

$$V_{\alpha\beta}(r) = 4\,\varepsilon_{\alpha\beta}\left[\left(\frac{\sigma_{\alpha\beta}}{r}\right)^{12} - \left(\frac{\sigma_{\alpha\beta}}{r}\right)^{6}\right], \tag{1}$$

where $\varepsilon_{AA} = 1.0$, $\varepsilon_{AB} = 1.5$, $\varepsilon_{BB} = 0.5$, $\sigma_{AA} = 1.0$, $\sigma_{AB} = 0.8$, $\sigma_{BB} = 0.88$, and $m_A = m_B$ [53]. The total number of atoms is $N = 60\,000$ and the cutoff radius is $r_{c,\alpha\beta} = 2.5\,\sigma_{\alpha\beta}$. Throughout the study, all physical quantities are reported in terms of the reduced units of length, mass, and energy, as follows: $\sigma = \sigma_{AA}$, $m = m_A$, and $\varepsilon = \varepsilon_{AA}$. In turn, the equations of motion for each atom were solved using the velocity Verlet algorithm with the integration time step $\Delta t_{MD} = 0.005\,\tau$, where $\tau = \sigma\sqrt{m/\varepsilon}$ is the characteristic LJ time [55,56].

The binary mixture was first placed in a periodic box of linear size $L = 36.84\,\sigma$ and equilibrated in a liquid phase at $T_{LJ} = 1.0\,\varepsilon/k_B$ and density $\rho = \rho_A + \rho_B = 1.2\,\sigma^{-3}$. In all simulations, the temperature was regulated via the Nosé–Hoover thermostat [55,56]. It was previously shown that the critical temperature of the KA model at $\rho = 1.2\,\sigma^{-3}$ is $T_g = 0.435\,\varepsilon/k_B$, where k_B is the Boltzmann constant [53]. After equilibration, the system was gradually cooled from $T_{LJ} = 1.0\,\varepsilon/k_B$ to $0.3\,\varepsilon/k_B$ with the rate $10^{-5}\varepsilon/k_B\tau$ at $\rho = 1.2\,\sigma^{-3}$. Then, the glass was further annealed by applying cyclic shear deformation along the xz plane at constant volume, as follows:

$$\gamma_{xz}(t) = \gamma_0 \sin(2\pi t/T), \tag{2}$$

where the oscillation period is $T = 5000\,\tau$, and the oscillation frequency is $\omega = 2\pi/T = 1.26 \times 10^{-3}\,\tau^{-1}$. The mechanical annealing included 5000 cycles with the strain amplitude $\gamma_0 = 0.035$ at the temperature $T_{LJ} = 0.30\,\varepsilon/k_B$ and density $\rho = 1.2\,\sigma^{-3}$. Note that it was recently shown for the KA model at $\rho = 1.2\,\sigma^{-3}$ that the strain amplitude $\gamma_0 = 0.035$ is below the critical value at the temperature $T_{LJ} = 0.30\,\varepsilon/k_B$, and the relaxation rate during cyclic loading with $\gamma_0 = 0.035$ is relatively fast [36,47]. The simulation of one sample during 5000 shear cycles took about 140 days using 40 processors in parallel.

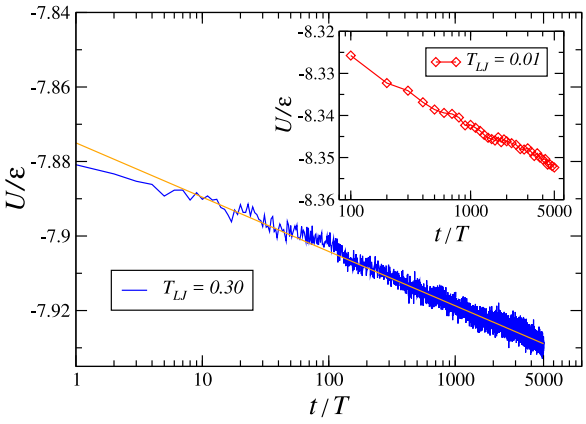

Fig. 1. (Color online) The potential energy at the end of each cycle (when strain is zero) as a function of the number of shear cycles with the strain amplitude $\gamma_0 = 0.035$ at the temperature $T_{LJ} = 0.30\,\varepsilon/k_B$ and density $\rho = 1.2\,\sigma^{-3}$. The oscillation period is $T = 5000\,\tau$. The orange curve $y = -7.875 - 0.0064 \cdot \ln(t/T)$ is plotted for reference. The inset shows the potential energy for selected cycles after the temperature was reduced to $T_{LJ} = 0.01\,\varepsilon/k_B$ during $10^4\,\tau$.

3. Results

It is well recognized by now that thermal and mechanical processing history strongly influences structural and mechanical properties of amorphous alloys [6]. In general, glasses that are more slowly cooled across the glass transition temperature become more stable (have lower energy states) and, under external deformation, exhibit a characteristic stress overshoot, which is a signature of a brittle material [57]. Furthermore, it was shown that periodic deformation during one shear cycle can lead either to further relaxation, if the strain amplitude is sufficiently small, or to rejuvenation when the strain amplitude is above a critical value [58]. Upon repeated cyclic loading, the yielding transition can be clearly detected at a certain strain amplitude, above which strain becomes localized along narrow bands; and, thus, oscillatory loading generally provides a better characterization of the yielding transition than continuous startup deformation [31]. On the other hand, in the presence of thermal fluctuations, the identification of the critical strain amplitude in a relatively large system is computationally challenging as it might require many cycles until yielding in the vicinity of the critical amplitude [47]. Therefore, in the present study, we first generate binary glasses in a broad range of energy states by means of mechanical annealing and then study how the yielding transition depends on the glass stability at finite temperature.

We first perform mechanical annealing at $T_{LJ} = 0.30\,\varepsilon/k_B$ and $\rho = 1.2\,\sigma^{-3}$ using cyclic shear with the strain amplitude $\gamma_0 = 0.035$ and present in Fig. 1 the potential energy minima after each cycle at zero strain as a function of the number of cycles. It can be clearly observed that the relaxation process continues during 5000 cycles without reaching a plateau level, and the maximum potential energy decrease is $\approx 0.05\,\varepsilon$. We comment that the logarithmic form of the relaxation process in Fig. 1 might be related to a slow defect annihilation in periodically driven systems of interacting particles in two dimensions in the presence of quenched disorder [59]. Furthermore, after selected number of cycles when strain is zero, the glass was linearly cooled from $T_{LJ} = 0.30\,\varepsilon/k_B$ to $0.01\,\varepsilon/k_B$ during the time interval $10^4\,\tau$ at constant volume. Thus, the inset in Fig. 1 shows the potential energy at $T_{LJ} = 0.01\,\varepsilon/k_B$ for the same number of cycles. It should be commented that such annealing procedure results in highly stable glasses with relatively low energy states. For comparison, rapidly quenched KA glasses under cyclic shear with strain amplitudes below the critical value $\gamma_0 \approx 0.067$ at $T_{LJ} = 0.01\,\varepsilon/k_B$ and $\rho = 1.2\,\sigma^{-3}$ settle at the lowest level $U \approx -8.29\,\varepsilon$ after one or two thousand cycles [39,45]. In addition, it was shown that

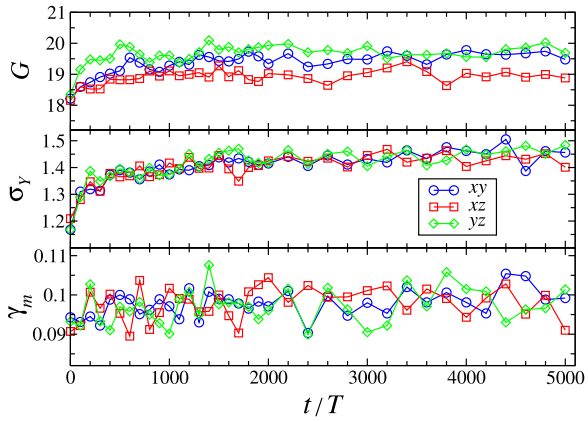

Fig. 2. (Color online) The shear modulus G and yielding peak σ_Y (both in units of $\epsilon\sigma^{-3}$) and shear strain of the yielding peak γ_m as a function of the number of annealing cycles at $T_{LJ} = 0.30\,\epsilon/k_B$. The data are reported for startup continuous shear deformation, which is imposed along the xy plane (blue circles), xz plane (red squares), and yz plane (green diamonds). The continuous deformation is applied at the constant strain rate $\dot{\gamma} = 10^{-5}\,\tau^{-1}$ at the temperature $T_{LJ} = 0.01\,\epsilon/k_B$ and density $\rho = 1.2\,\sigma^{-3}$. See text for details.

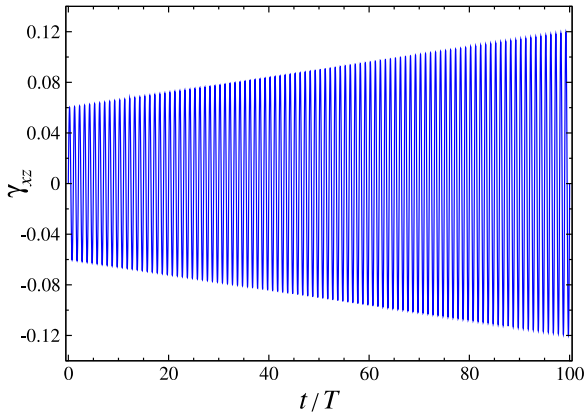

Fig. 3. (Color online) The applied shear strain along the xz plane during 100 cycles with the oscillation period $T = 5000\,\tau$. The strain amplitude is varied linearly from $\gamma_0 = 0.06$ to 0.12 in order to detect the yield strain in stable glasses at the temperature $T_{LJ} = 0.01\,\epsilon/k_B$.

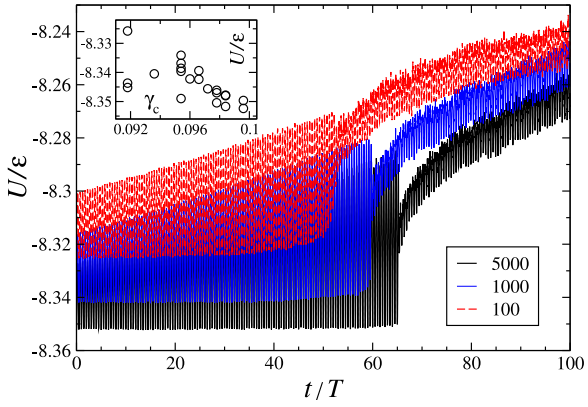

Fig. 4. (Color online) The time dependence of the potential energy, U/ϵ, for glasses that were initially annealed during 100, 1000, and 5000 shear cycles at $T_{LJ} = 0.30\,\epsilon/k_B$. The strain profile shown in Fig. 3 was applied at $T_{LJ} = 0.01\,\epsilon/k_B$ and $\rho = 1.2\,\sigma^{-3}$. The oscillation period is $T = 5000\,\tau$. The inset shows the critical strain amplitude as a function of the potential energy before the shear deformation, Eq. (3), was applied.

periodic shear with $\gamma_0 = 0.06$ at $0.01\,\epsilon/k_B$ and $1.2\,\sigma^{-3}$ does not lead to relaxation below $U \approx -8.31\,\epsilon$ [49].

Next, the mechanical properties of stable glasses are probed during startup continuous shear deformation protocol. The continuous deformation was applied at the constant strain rate $\dot{\gamma} = 10^{-5}\,\tau^{-1}$ along the xy, xz, and yz planes. The results for the shear modulus, G, yielding peak, σ_Y, and its strain, γ_m, are reported in Fig. 2. In each case, the shear modulus was computed from the linear slope of the stress–strain curve when $\gamma \leqslant 0.01$, and the yielding peak and the corresponding strain were determined from the local maximum of the shear stress for $\gamma \leqslant 0.20$. The data are rather scattered as simulations were carried our only for one sample. It can be seen in Fig. 2 that both G and σ_Y increase noticeably during the first 1000 cycles and then level out to plateau levels. Moreover, the shear modulus exhibits a slight directional anisotropy, and G is smaller along the xz plane that was used for mechanical annealing at $T_{LJ} = 0.30\,\epsilon/k_B$. It was previously shown that the effect of anisotropy in mechanical properties is reduced when the direction of periodic loading is alternated in two or three spatial dimensions [39]. Finally, as shown in the lower panel in Fig. 2, the strain of the yielding peak remains roughly independent of the cycle number.

Recent MD studies have demonstrated that the yielding behavior under oscillatory shear deformation is qualitatively different in highly stable glasses [44,48]. In particular, it was found that sufficiently well annealed glasses do not relax further when subjected to periodic shear with a strain amplitude below a critical value, and the critical strain amplitude becomes higher for deeply annealed glasses [44,48]. The numerical evaluation of the critical strain amplitude using athermal quasistatic shear protocol involves a series of simulations in the vicinity of the critical value. At zero temperature, periodic shear at smaller amplitudes leads to limit cycles where trajectories of all atoms are exactly reversible, whereas above the critical strain amplitude, the yielding transition is accompanied by a discontinuous energy change due to formation of a shear band [44,48]. However, when the system size is large and the temperature is finite, the precise determination of the critical strain amplitude for stable glasses becomes more difficult computationally. For example, periodic loading of a relatively large system ($N = 60\,000$) at two temperatures well below T_g required thousands of cycles in order to estimate critical strain amplitudes for glasses with different degrees of stability [47]. Moreover, at fixed strain amplitudes, the system dynamics remained nearly reversible during thousands of cycles for highly stable glasses, leaving the possibility of yielding under continued loading [47].

In the present study, we introduce a deformation protocol where the strain amplitude is gradually varied across a critical strain amplitude. It was shown previously that the critical strain amplitude for poorly annealed binary glasses is $\gamma_0 \approx 0.067$ at $T_{LJ} = 0.01\,\epsilon/k_B$ and $\rho = 1.2\,\sigma^{-3}$ and that better annealed glasses at the same conditions do not yield at $\gamma_0 = 0.06$ [39,45,49]. Therefore, the strain amplitude is set to vary linearly from $\gamma_0 = 0.06$ to 0.12 during 100 cycles, as follows:

$$\gamma_{xz}(t) = 0.06\,(1 + t/100\,T)\sin(2\pi t/T), \tag{3}$$

where the oscillation period is the same, *i.e.*, $T = 5000\,\tau$. The variation of strain as a function of time is shown in Fig. 3. In what follows, this deformation protocol was applied at the temperature $T_{LJ} = 0.01\,\epsilon/k_B$ and density $\rho = 1.2\,\sigma^{-3}$.

The time dependence of the potential energy subjected to the deformation protocol, given by Eq. (3), is presented in Fig. 4 for binary glasses that were initially annealed during 100, 1000, and 5000 cycles at $T_{LJ} = 0.30\,\epsilon/k_B$. As is evident, the yielding transition, marked by the abrupt energy change, occurs after larger number of cycles for more stable glasses. Note that for the most stable glass (see the black curve in Fig. 4), the potential energy minima at zero strain remain nearly constant during the first 65 cycles, implying nearly reversible dynamics,

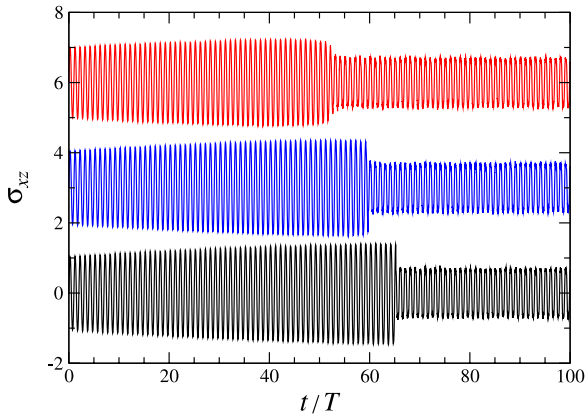

Fig. 5. (Color online) The shear stress σ_{xz} (in units of $\varepsilon\sigma^{-3}$) during 100 cycles when the shear strain is given by Eq. (3). The glasses were initially annealed during 100 cycles (red curve), 1000 cycles (blue curve), and 5000 cycles (black curve) at $T_{LJ} = 0.30\,\varepsilon/k_B$ and then cooled to $0.01\,\varepsilon/k_B$. For clarity, the data were displaced vertically by $6.0\,\varepsilon\sigma^{-3}$ (red curve) and by $3.0\,\varepsilon\sigma^{-3}$ (blue curve). The period of oscillation is $T = 5000\,\tau$.

followed by a sudden energy increase during the next cycle. By contrast, in the case of the least stable glass (indicated by the red curve in Fig. 4), the potential energy minima gradually increase during 52 cycles via strain-induced localized plastic rearrangements (discussed below), until the yielding transition occurs during the 53-rd cycle. Also, in all cases shown in Fig. 4, the potential energy during the first 11 cycles (when the strain amplitude is below $\gamma_0 \approx 0.067$) does not decrease, indicating that glasses were sufficiently well annealed. In addition, it was previously shown that the sharp increase and gradual saturation of the potential energy after the yielding transition is due to increasing width of a shear band under periodic loading [42].

Further, the critical strain amplitude as a function of the potential energy of undeformed glasses (at $T_{LJ} = 0.01\,\varepsilon/k_B$ and $\rho = 1.2\,\sigma^{-3}$) is plotted in the inset to Fig. 4. Despite data scattering, it can be clearly observed that the critical strain amplitude increases in more stable, lower-energy glasses. These results are in agreement with the conclusions obtained for periodically deformed zero-temperature glasses under athermal quasistatic shear [44,48]. It should also be commented that the values of γ_c reported in the inset to Fig. 4 represent upper bounds for the critical strain amplitudes. For example, it is estimated that $\gamma_c \approx 0.092$ for the glass annealed during 100 cycles at $T_{LJ} = 0.30\,\varepsilon/k_B$ (*i.e.*, $U = -8.326\,\varepsilon$ in the inset to Fig. 4). However, it was previously shown that the same sample yielded after about 100 cycles at a smaller strain amplitude $\gamma_0 = 0.08$ at $T_{LJ} = 0.01\,\varepsilon/k_B$ and $\rho = 1.2\,\sigma^{-3}$, as shown by the red curve in Fig. 7 in Ref. [47].

In addition, the variation of the shear stress under periodic strain given by Eq. (3) is reported in Fig. 5 for the same samples as in Fig. 4. Note that the colorcode is the same, and the data for the first two samples are displaced vertically for clarity. The same trends as for the potential energy can be observed for the shear stress in Fig. 5. Namely, upon increasing glass stability, the yielding transition becomes more abrupt and it occurs at higher strain amplitudes. After the yielding transition, a shear band is formed across the whole system, and, as a result, the stress amplitude is largely independent of the strain amplitude.

The spatial and temporal analysis of plastic deformation near the yielding transition can be performed by identifying the so-called nonaffine displacements of atoms with respect to their neighbors. To briefly remind, the nonaffine measure associated with an atom i is calculated using the matrix $\mathbf{J}_i$ which linearly transforms a group of neighboring atoms and at the same time minimizes the following expression:

$$D^2(t,\Delta t) = \frac{1}{N_i}\sum_{j=1}^{N_i}\Big\{\mathbf{r}_j(t+\Delta t) - \mathbf{r}_i(t+\Delta t) - \mathbf{J}_i\big[\mathbf{r}_j(t) - \mathbf{r}_i(t)\big]\Big\}^2, \qquad (4)$$

where Δt is the time interval between two configurations of atoms, and the sum is taken over all atoms located within $1.5\,\sigma$ from the position of the ith atom at $\mathbf{r}_i(t)$ [60]. In general, a local plastic deformation is detected when an atom escapes a cage of its neighbors, and, when the time interval Δt is suitably chosen, the nonaffine measure given by Eq. (4) becomes greater than the cage size. Typically, a plastic event in a deformed disordered solid involves a group of atoms with relatively large nonaffine displacements. More recently, the collective behavior of atoms with large nonaffine displacements was investigated in disordered solids during elastostatic loading [61,62] as well as startup continuous [63–69] and oscillatory shear [28,34,35,39,42,43,45,47,49] deformation.

The snapshots of atomic configurations during 8 consecutive cycles near the yielding transition are displayed in Figs. 6 and 7 for the binary glass that was initially annealed during 100 cycles at $T_{LJ} = 0.30\,\varepsilon/k_B$. For clarity, only atoms with relatively large nonaffine displacements during one cycle, *i.e.*, $\Delta t = T$ in Eq. (4), $D^2(nT,T) > 0.04\,\sigma^2$ are shown. Here, $n = 46,\ldots,53$, and the nonaffine displacements in each case are computed with respect to atomic configurations at zero strain. It can be clearly observed that upon approaching the yielding transition, the nonaffine displacements form compact clusters that become comparable to the system size. The yielding transition occurs during the 53-rd cycle, when a shear band is formed along the xy plane, as shown in Fig. 7 (c). The accumulation of plastic activity and the formation of a narrow band where strain is localized correlates well with the variation of the potential energy and shear stress (shown by the red curves in Figs. 4 and 5).

The results in Figs. 4 and 5 have also revealed that the yielding transition becomes more abrupt in better annealed glasses. Thus, the time evolution of plastic deformation across the yielding transition is presented in Figs. 8 and 9 for glasses that were annealed at $T_{LJ} = 0.30\,\varepsilon/k_B$ for 1000 and 5000 cycles, respectively. In particular, it can be seen in Fig. 8 that the yielding transition during the 60-th cycle is preceded by the appearance of several compact clusters of atoms with large nonaffine displacements that later coalesce to form a shear band along the xy plane. Lastly, the yielding of the highly stable glass is associated with a sudden formation of a shear band during the 66-th cycle along the yz plane, but the location and orientation of the band is difficult to predict based on small isolated clusters of atoms with large nonaffine displacements (see Fig. 9). We thus conclude that the size of plastic rearrangements preceding the formation of a shear band is reduced for more stable glasses.

4. Conclusions

In summary, we carried out molecular dynamics simulations to study the effect of glass stability on yielding transition during time periodic shear deformation. The model glass is a binary mixture of two types of atoms with strongly non-additive interaction, which suppresses crystallization upon cooling across the glass transition temperature. The binary glasses in a broad range of energy states were first prepared via periodic shear deformation below the glass transition temperature during thousands of cycles, and then cooled deep into the glass phase. It was shown that both the shear modulus and the yielding peak during startup continuous deformation increase towards plateau levels for deeply annealed glasses, whereas the yield strain remains relatively insensitive to the degree of annealing. Furthermore, in order to evaluate a critical strain amplitude, a deformation protocol with slowly varying strain amplitude was introduced. It was found that more stable glasses at finite temperature undergo a yield transition at higher strain amplitudes. Lastly, the spatial analysis of clusters of atoms with large nonaffine displacements illustrated that the yielding transition becomes more abrupt in deeply annealed glasses.

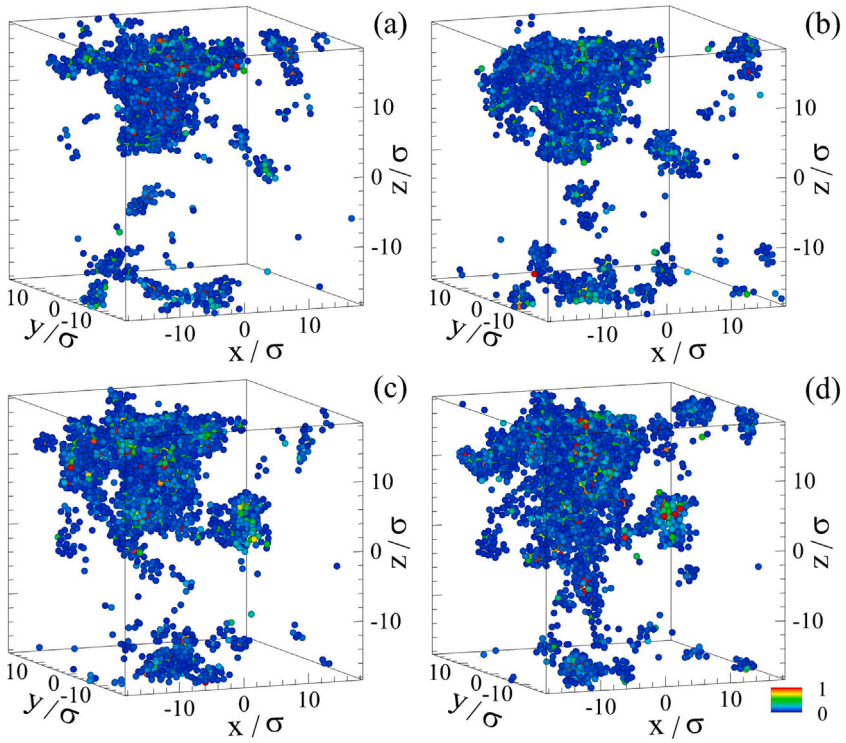

Fig. 6. (Color online) The series of snapshots of atoms with large nonaffine displacements after one shear cycle with the period $T = 5000\,\tau$, when the strain is varied linearly as shown in Fig. 3. The glass was initially annealed during 100 cycles at $T_{LJ} = 0.30\,\epsilon/k_B$ and then cooled to $0.01\,\epsilon/k_B$. The nonaffine measure, as defined by Eq. (4), is (a) $D^2(46\,T, T) > 0.04\,\sigma^2$, (b) $D^2(47\,T, T) > 0.04\,\sigma^2$, (c) $D^2(48\,T, T) > 0.04\,\sigma^2$, and (d) $D^2(49\,T, T) > 0.04\,\sigma^2$. The legend color indicates the magnitude of D^2.

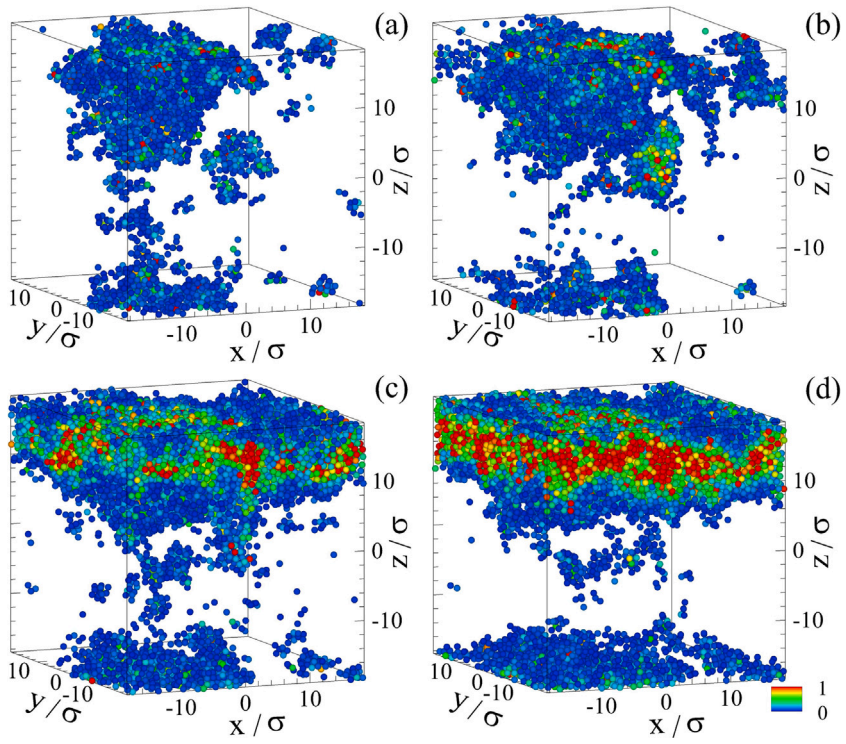

Fig. 7. (Color online) The atomic configurations after one shear cycle with the period $T = 5000\,\tau$ for the same sample as in Fig. 6. The mechanical response is indicated by the red curves in Figs. 4 and 5. The nonaffine quantity is (a) $D^2(50\,T, T) > 0.04\,\sigma^2$, (b) $D^2(51\,T, T) > 0.04\,\sigma^2$, (c) $D^2(52\,T, T) > 0.04\,\sigma^2$, and (d) $D^2(53\,T, T) > 0.04\,\sigma^2$. The magnitude of D^2 is specified in the legend.

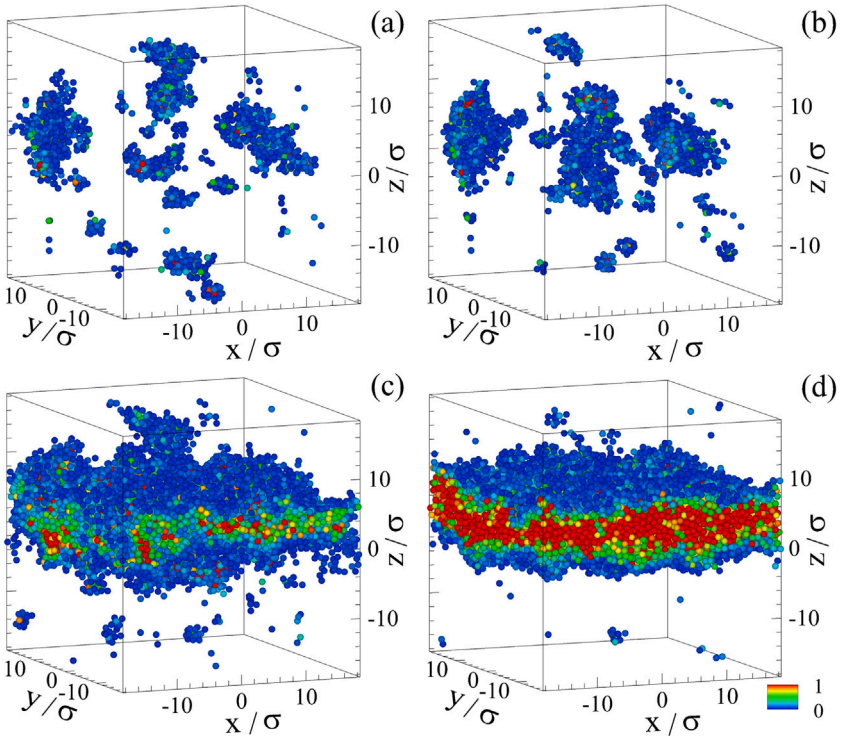

Fig. 8. (Color online) The consecutive snapshots of a glass that was initially annealed during 1000 cycles at $T_{LJ} = 0.30\,\epsilon/k_B$, then cooled to $0.01\,\epsilon/k_B$, and subjected to periodic shear given by Eq. (3). The corresponding U and σ_{xz} are denoted by the blue curves in Figs. 4 and 5. The nonaffine measure is (a) $D^2(57\,T, T) > 0.04\,\sigma^2$, (b) $D^2(58\,T, T) > 0.04\,\sigma^2$, (c) $D^2(59\,T, T) > 0.04\,\sigma^2$, and (d) $D^2(60\,T, T) > 0.04\,\sigma^2$. The magnitude of D^2 is denoted by color in the legend.

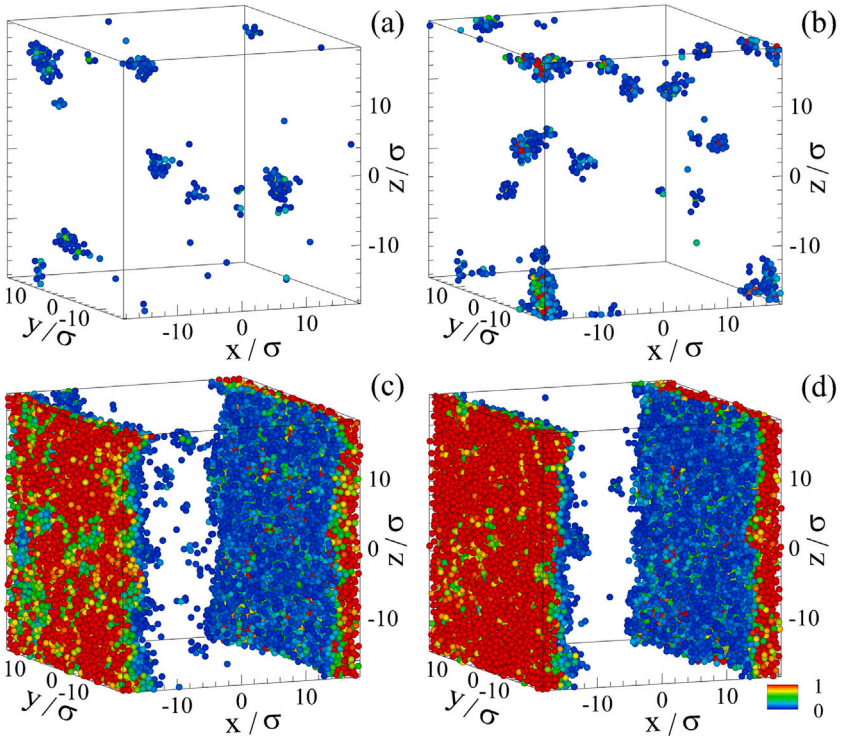

Fig. 9. (Color online) Zero-strain configurations of a binary glass that was initially annealed during 5000 cycles at $T_{LJ} = 0.30\,\epsilon/k_B$ and then cooled to $0.01\,\epsilon/k_B$. The same deformation protocol is denoted by the black curves in Figs. 4 and 5. The nonaffine measure is (a) $D^2(63\,T, T) > 0.04\,\sigma^2$, (b) $D^2(64\,T, T) > 0.04\,\sigma^2$, (c) $D^2(65\,T, T) > 0.04\,\sigma^2$, and (d) $D^2(66\,T, T) > 0.04\,\sigma^2$. The legend denotes the magnitude of D^2.

Declaration of competing interest

The authors declare that they have no known competing financial interests or personal relationships that could have appeared to influence the work reported in this paper.

Acknowledgments

Financial support from the National Science Foundation (CNS-1531923) is gratefully acknowledged. The article was prepared within the framework of the HSE University Basic Research Program and funded in part by the Russian Academic Excellence Project '5-100'. The simulations were performed at Wright State University's Computing Facility and the Ohio Supercomputer Center using the LAMMPS code developed at Sandia National Laboratories [56].

References

[1] Y.Q. Cheng, E. Ma, Atomic-level structure and structure–property relationship in metallic glasses, Prog. Mater. Sci. 56 (2011) 379.
[2] P. Yiu, W. Diyatmika, N. Bonninghoff, Y.-C. Lu, B.-Z. Lai, J.P. Chu, Thin film metallic glasses: Properties, applications and future, J. Appl. Phys. 127 (2020) 030901.
[3] A. Loye, H.-K. Kwon, D. Dellal, R. Ojeda, S. Lee, R. Davis, N. Nagle, P.G. Doukas, J. Schroers, F.Y. Lee, T.R. Kyriakides, Biocompatibility of platinum-based bulk metallic glass in orthopedic applications, Biomed. Mater. 16 (2021) 045018.
[4] F. Spaepen, A microscopic mechanism for steady state inhomogeneous flow in metallic glasses, Acta Metall. 25 (1977) 407.
[5] A.S. Argon, Plastic deformation in metallic glasses, Acta Metall. 27 (1979) 47.
[6] Y. Sun, A. Concustell, A.L. Greer, Thermomechanical processing of metallic glasses: Extending the range of the glassy state, Nat. Rev. Mater. 1 (2016) 16039.
[7] S.V. Ketov, Y.H. Sun, S. Nachum, Z. Lu, A. Checchi, A.R. Beraldin, H.Y. Bai, W.H. Wang, D.V. Louzguine-Luzgin, M.A. Carpenter, A.L. Greer, Rejuvenation of metallic glasses by non-affine thermal strain, Nature 524 (2015) 200.
[8] W. Guo, J. Saida, M. Zhao, S. Lu, S. Wu, Rejuvenation of Zr-based bulk metallic glass matrix composite upon deep cryogenic cycling, Mater. Lett. 247 (2019) 135.
[9] N.V. Priezjev, The effect of cryogenic thermal cycling on aging, rejuvenation, and mechanical properties of metallic glasses, J. Non-Cryst. Solids 503 (2019) 131.
[10] Q.-L. Liu, N.V. Priezjev, The influence of complex thermal treatment on mechanical properties of amorphous materials, Comput. Mater. Sci. 161 (2019) 93.
[11] N.V. Priezjev, Potential energy states and mechanical properties of thermally cycled binary glasses, J. Mater. Res. 34 (2019) 2664.
[12] M. Samavatian, R. Gholamipour, A.A. Amadeh, S. Mirdamadi, Correlation between plasticity and atomic structure evolution of a rejuvenated bulk metallic glass, Metall. Mater. Trans. A 50 (2019) 4743.
[13] N.V. Priezjev, Atomistic modeling of heat treatment processes for tuning the mechanical properties of disordered solids, J. Non-Cryst. Solids 518 (2019) 128.
[14] J. Ketkaew, R. Yamada, H. Wang, D. Kuldinow, B.S. Schroers, W. Dmowski, T. Egami, J. Schroers, The effect of thermal cycling on the fracture toughness of metallic glasses, Acta Mater. 184 (2020) 100.
[15] C.M. Meylan, F. Papparotto, S. Nachum, J. Orava, M. Miglierini, V. Basykh, J. Ferenc, T. Kulik, A.L. Greer, Stimulation of shear-transformation zones in metallic glasses by cryogenic thermal cycling, J. Non-Cryst. Solids 584 (2020) 120299.
[16] W. Zhang, Q.C. Xiang, C.Y. Ma, Y.L. Ren, K.Q. Qiu, Relaxation-to-rejuvenation transition of a Ce-based metallic glass by quenching/cryogenic treatment performed at sub-Tg, J. Alloys Compd. 825 (2020) 153997.
[17] B. Shang, W. Wang, A.L. Greer, P. Guan, Atomistic modelling of thermal-cycling rejuvenation in metallic glasses, Acta Mater. 213 (2021) 116952.
[18] M. Bruns, M. Hassani, F. Varnik, A. Hassanpour, S. Divinski, G. Wilde, Decelerated aging in metallic glasses by low temperature thermal cycling, Phys. Rev. Res. 3 (2021) 013234.
[19] R.M.O. Mota, E.T. Lund, S. Sohn, D.J. Browne, D.C. Hofmann, S. Curtarolo, A. van de Walle, J. Schroers, Enhancing ductility in bulk metallic glasses by straining during cooling, Commun. Mater. 2 (2021) 23.
[20] N.V. Priezjev, Cooling under applied stress rejuvenates amorphous alloys and enhances their ductility, Metals 11 (2021) 67.
[21] Y.C. Lo, H.S. Chou, Y.T. Cheng, J.C. Huang, J.R. Morris, P.K. Liaw, Structural relaxation and self-repair behavior in nano-scaled Zr-Cu metallic glass under cyclic loading: Molecular dynamics simulations, Intermetallics 18 (2010) 954.
[22] N.V. Priezjev, Heterogeneous relaxation dynamics in amorphous materials under cyclic loading, Phys. Rev. E 87 (2013) 052302.
[23] D. Fiocco, G. Foffi, S. Sastry, Oscillatory athermal quasistatic deformation of a model glass, Phys. Rev. E 88 (2013) 020301(R).
[24] I. Regev, T. Lookman, C. Reichhardt, Onset of irreversibility and chaos in amorphous solids under periodic shear, Phys. Rev. E 88 (2013) 062401.
[25] I. Regev, J. Weber, C. Reichhardt, K.A. Dahmen, T. Lookman, Reversibility and criticality in amorphous solids, Nature Commun. 6 (2015) 8805.
[26] J. Luo, K. Dahmen, P.K. Liaw, Y. Shi, Low-cycle fatigue of metallic glass nanowires, Acta Mater. 87 (2015) 225.
[27] Y.F. Ye, S. Wang, J. Fan, C.T. Liu, Y. Yang, Atomistic mechanism of elastic softening in metallic glass under cyclic loading revealed by molecular dynamics simulations, Intermetallics 68 (2016) 5.
[28] N.V. Priezjev, Reversible plastic events during oscillatory deformation of amorphous solids, Phys. Rev. E 93 (2016) 013001.
[29] T. Kawasaki, L. Berthier, Macroscopic yielding in jammed solids is accompanied by a non-equilibrium first-order transition in particle trajectories, Phys. Rev. E 94 (2016) 022615.
[30] N.V. Priezjev, Nonaffine rearrangements of atoms in deformed and quiescent binary glasses, Phys. Rev. E 94 (2016) 023004.
[31] P. Leishangthem, A.D.S. Parmar, S. Sastry, The yielding transition in amorphous solids under oscillatory shear deformation, Nature Commun. 8 (2017) 14653.
[32] N.V. Priezjev, Collective nonaffine displacements in amorphous materials during large-amplitude oscillatory shear, Phys. Rev. E 95 (2017) 023002.
[33] M. Fan, M. Wang, K. Zhang, Y. Liu, J. Schroers, M.D. Shattuck, C.S. O'Hern, The effects of cooling rate on particle rearrangement statistics: Rapidly cooled glasses are more ductile and less reversible, Phys. Rev. E 95 (2017) 022611.
[34] N.V. Priezjev, Molecular dynamics simulations of the mechanical annealing process in metallic glasses: Effects of strain amplitude and temperature, J. Non-Cryst. Solids 479 (2018) 42.
[35] N.V. Priezjev, The yielding transition in periodically sheared binary glasses at finite temperature, Comput. Mater. Sci. 150 (2018) 162.
[36] P. Das, A.D.S. Parmar, S. Sastry, Annealing glasses by cyclic shear deformation, 2018, arXiv:1805.12476.
[37] N.V. Priezjev, Slow relaxation dynamics in binary glasses during stress-controlled, tension-compression cyclic loading, Comput. Mater. Sci. 153 (2018) 235.
[38] A.D.S. Parmar, S. Kumar, S. Sastry, Strain localization above the yielding point in cyclically deformed glasses, Phys. Rev. X 9 (2019) 021018.
[39] N.V. Priezjev, Accelerated relaxation in disordered solids under cyclic loading with alternating shear orientation, J. Non-Cryst. Solids 525 (2019) 119683.
[40] S. Li, P. Huang, F. Wang, Rejuvenation saturation upon cyclic elastic loading in metallic glass, Comput. Mater. Sci. 166 (2019) 318.
[41] Z.-Y. Zhou, H.-L. Peng, H.-B. Yu, Structural origin for vibration-induced accelerated aging and rejuvenation in metallic glasses, J. Chem. Phys. 150 (2019) 204507.
[42] N.V. Priezjev, Shear band formation in amorphous materials under oscillatory shear deformation, Metals 10 (2020) 300.
[43] P.K. Jana, N.V. Priezjev, Structural relaxation in amorphous materials under cyclic tension-compression loading, J. Non-Cryst. Solids 540 (2020) 120098.
[44] W.-T. Yeh, M. Ozawa, K. Miyazaki, T. Kawasaki, L. Berthier, Glass stability changes the nature of yielding under oscillatory shear, Phys. Rev. Lett. 124 (2020) 225502.
[45] N.V. Priezjev, Alternating shear orientation during cyclic loading facilitates yielding in amorphous materials, J. Mater. Eng. Perform. 29 (2020) 7328.
[46] T. Kawasaki, A. Onuki, Acoustic resonance in periodically sheared glass: damping due to plastic events, Soft Matter 16 (2020) 9357.
[47] N.V. Priezjev, A delayed yielding transition in mechanically annealed binary glasses at finite temperature, J. Non-Cryst. Solids 548 (2020) 120324.
[48] H. Bhaumik, G. Foffi, S. Sastry, The role of annealing in determining the yielding behavior of glasses under cyclic shear deformation, Proc. Natl. Acad. Sci. USA 118 (2021) 2100227118.
[49] N.V. Priezjev, Accessing a broader range of energy states in metallic glasses by variable-amplitude oscillatory shear, J. Non-Cryst. Solids 560 (2021) 120746.
[50] C. Liu, E.E. Ferrero, E.A. Jagla, K. Martens, A. Rosso, L. Talon, Oscillatory quasistatic shear deformation of amorphous materials: a mesoscopic approach, 2021, arXiv:2012.15310.
[51] N.V. Priezjev, Shear band healing in amorphous materials by small-amplitude oscillatory shear deformation, J. Non-Cryst. Solids 566 (2021) 120874.
[52] B.L. Brown, C. Reichhardt, C.J.O. Reichhardt, Reversible to irreversible transitions in periodically driven skyrmion systems, New J. Phys. 21 (2019) 013001.
[53] W. Kob, H.C. Andersen, Testing mode-coupling theory for a supercooled binary Lennard-Jones mixture: The van Hove correlation function, Phys. Rev. E 51 (1995) 4626.
[54] T.A. Weber, F.H. Stillinger, Local order and structural transitions in amorphous metal–metalloid alloys, Phys. Rev. B 31 (1985) 1954.
[55] M.P. Allen, D.J. Tildesley, Computer Simulation of Liquids, Clarendon, Oxford, 1987.
[56] S.J. Plimpton, Fast parallel algorithms for short-range molecular dynamics, J. Comput. Phys. 117 (1995) 1.
[57] T. Egami, T. Iwashita, W. Dmowski, Mechanical properties of metallic glasses, Metals 3 (2013) 77.
[58] D.J. Lacks, M.J. Osborne, Energy landscape picture of overaging and rejuvenation in a sheared glass, Phys. Rev. Lett. 93 (2004) 255501.

[59] C. Reichhardt, C.J.O. Reichhardt, Coarsening of topological defects in oscillating systems with quenched disorder, Phys. Rev. E 73 (2006) 046122.
[60] M.L. Falk, J.S. Langer, Dynamics of viscoplastic deformation in amorphous solids, Phys. Rev. E 57 (1998) 7192.
[61] N.V. Priezjev, Aging and rejuvenation during elastostatic loading of amorphous alloys: A molecular dynamics simulation study, Comput. Mater. Sci. 168 (2019) 125.
[62] N.V. Priezjev, Accelerated rejuvenation in metallic glasses subjected to elastostatic compression along alternating directions, J. Non-Cryst. Solids 556 (2021) 120562.
[63] G.P. Shrivastav, P. Chaudhuri, J. Horbach, Yielding of glass under shear: A directed percolation transition precedes shear-band formation, Phys. Rev. E 94 (2016) 042605.
[64] A. Ghosh, Z. Budrikis, V. Chikkadi, A.L. Sellerio, S. Zapperi, P. Schall, Direct observation of percolation in the yielding transition of colloidal glasses, Phys. Rev. Lett. 118 (2017) 148001.
[65] R. Jana, L. Pastewka, Correlations of non-affine displacements in metallic glasses through the yield transition, J. Phys.: Mater. 2 (2019) 045006.
[66] N.V. Priezjev, The effect of thermal history on the atomic structure and mechanical properties of amorphous alloys, Comput. Mater. Sci. 174 (2020) 109477.
[67] N.V. Priezjev, Spatiotemporal analysis of nonaffine displacements in disordered solids sheared across the yielding point, Metall. Mater. Trans. A 51 (2020) 3713.
[68] M. Singh, M. Ozawa, L. Berthier, Brittle yielding of amorphous solids at finite shear rates, Phys. Rev. Mater. 4 (2020) 025603.
[69] R. Shi, P. Xiao, R. Yang, Y. Bai, Atomic-level structural identification for prediction of localized shear deformation in metallic glasses, Int. J. Solids Struct. 191 (2020) 363.